Silicon dual-ring resonator-based push-pull modulators

Xiaomeng Sun*[a], Linjie Zhou[b], Matthias Jäger[a], Despoina Petousi[c], Lars Zimmermann[a,c], and Klaus Petermann[a]
[a]Fachgebiet Hochfrequenztechnik, Technische Universität Berlin, Berlin 10587, Germany;
[b]State Key Laboratory of Advanced Optical Communication Systems and Networks, Department of Electronic Engineering, Shanghai Jiao Tong University, Shanghai, 200240, China;
[c]IHP, Im Technologiepark 25, 15236 Frankfurt (Oder), Germany
* xiaomeng.sun@tu-berlin.de

ABSTRACT

Two types of silicon dual-ring resonator-based high-speed optical modulators are proposed. With two microring resonators cascaded either in series or in parallel, the transmission spectrum evolves from a deep notch to a sharp peak with the resonators operating in a push-pull manner. The frequency chirp of the modulated signals can be highly suppressed by choosing a proper working wavelength.

Keywords: silicon photonics, waveguides, microresonators, modulator, electro-optical devices, electromagnetically induced transparency

1. INTRODUCTION

Electro-optical silicon modulators [1-6] are a key element in photonic integrated circuits (PICs) for optical telecommunications and interconnects. Multiple silicon modulators based on the free-carrier dispersion effect have been demonstrated theoretically and experimentally, among which Mach-Zehnder modulators (MZM) have drawn much attention due to the advantages of broad optical bandwidth, low chirp (in a push-pull configuration), and fast speed. However, MZMs are relatively large with a typical length of about several millimeters or even centimeters to achieve a high modulation depth.

For ultra-compact modulators, microring resonators are preferable to Mach-Zehnder interferometers (MZI) due to their lower footprint. However, there is a tradeoff between the optical bandwidth and depth for a conventional microring modulator under a given drive voltage. Furthermore, it is challenging to obtain chirp-free modulation with the refractive index modulation directly imposed on the ring waveguide. Cascaded microring resonators open the possibility for further increasing the overall modulation performance [7]. The resonance frequencies for all resonators can be accurately aligned via active tuning. In [6], a compact silicon coupled-ring modulator has been proposed, in which only one ring is actively driven. To enable high modulation speeds, it is designed heavily over-coupled to the waveguide.

In this paper, we propose and analyze two types of push-pull silicon microring resonator-based modulators. In one configuration where the two rings are connected in series with one ring on through transmission and the other on drop transmission, the output power contrast between the "on" and "off" states is enhanced due to the interaction of resonances from the two rings, leading to a high modulation depth. The optical bandwidth for a given modulation depth is wider than that of a single ring modulator. The frequency chirp of the modulated signal can be highly suppressed by operating both rings at the critical coupling point around resonances. In the parallel configuration where the two rings are coupled with two parallel bus waveguides, the electromagnetically induced transparency (EIT)-like effect [8, 9] is generated its EIT peak power dependent on the relative resonance wavelengths of the two rings. By push-pull modulation of the two rings, the EIT peak is varied, leading to an intensity modulation with a low drive voltage. The frequency chirp of the modulated signals is eliminated as the two rings always shift in the opposite wavelength directions. The chirp-free modulation is an essential requirement for long-haul optical transmission. Our two dual-ring modulator configurations provide a solution for ring modulators to be used in optical telecommunications.

Silicon Photonics XI, edited by Graham T. Reed, Andrew P. Knights, Proc. of SPIE Vol. 9752, 975208
 · doi: 10.1117/12.2218876

2. DUAL-RING MODULATOR IN A SERIAL CONFIGURATION

In the serial configuration, there are two type of connections with the second ring connected either to the through-port or to the drop-port of the first ring as shown in Figs. 1(a) and 1(b), respectively. PN junctions are embedded in each ring for refractive index modulation via the free-carrier plasma dispersion effect in silicon. t_i and k_i with i= 1, 2, 3, 4 are the transmission and coupling coefficients of the four directional couplers, respectively, a is the resonator loss factor, and r is the ring radius. The two ring resonators (R_1 and R_2) are designed with the same dimensions.

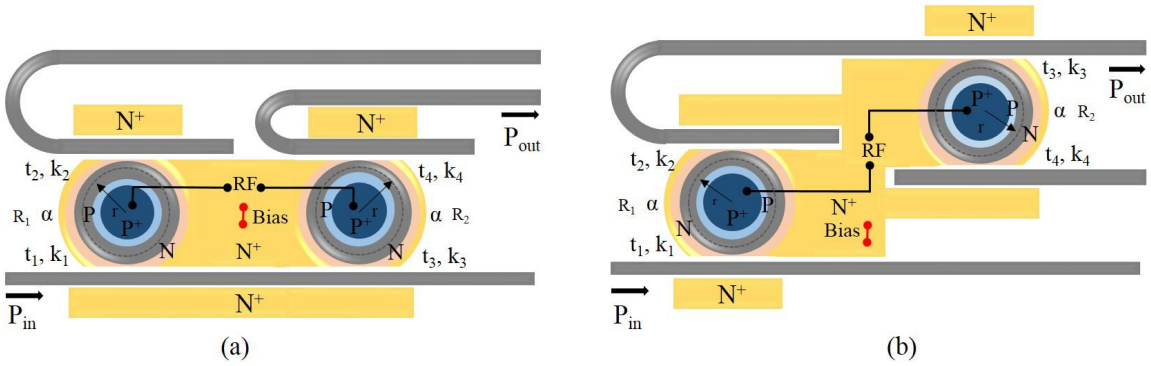

Figure 1. Schematic illustration of the coupled dual-ring resonators in the series configuration. The second ring is connected to the (a) through-port of the first ring, (b) drop-port of the first ring.

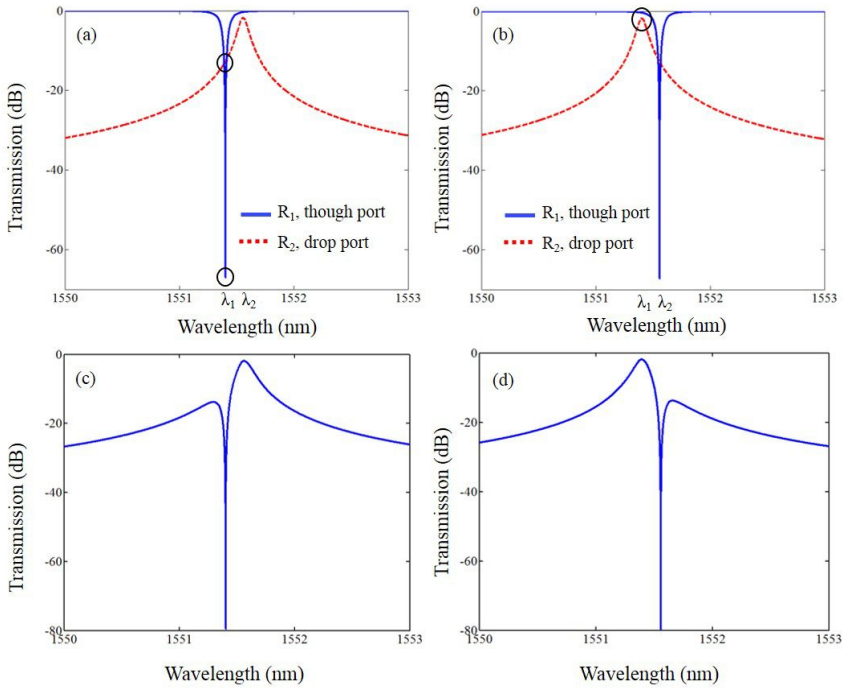

Figure 2. (a) and (b) Optical transmission spectra of individual rings in the serial configuration under push-pull modulation. (c) and (d) The overall spectrum of the output port. (a) and (c) show one modulation state with R_1 blue-shifted and R_2 red-shifted; (b) and (d) the other state with R_1 red-shifted and R_2 blue-shifted.

The performances of both realizations are identical, so we analyze the dual-ring modulator shown in Fig. 1(a) as an example. The device parameters are set as a=0.995, r =10 μm, t_2=t_4=0.98. Both rings here are designed to approach critical coupling. For simplicity, critical coupling is assumed to be satisfied in both modulation states in the calculations, and we have $t_1 = t_3 = at_2 = at_4$. As the two rings are identical, they resonate at the same wavelength without RF drive. The waveguide refractive index change (Δn_{eff}) is assumed to be ±0.0002 during the push-pull modulation. At one modulation state, the resonance of the first ring is blue-shifted to λ_1 while the resonance of the second ring is red-shifted to λ_2, as

shown in Fig. 2(a). At the other modulation state, the resonance shift is reversed and the spectra are shown in Fig. 2(b). The output response of the cascaded rings is the multiplication of individual ring transfer functions. Therefore, the deep notch at λ_1 in Fig. 2(c) results in the "0" level of the modulated signal. The transmission of both rings becomes high at λ_1 at the other modulation state, leading to the "1" level of the modulated signal as shown in Fig. 2(d). A similar response with an inverted modulation waveform could be observed when the operation wavelength is set to λ_2.

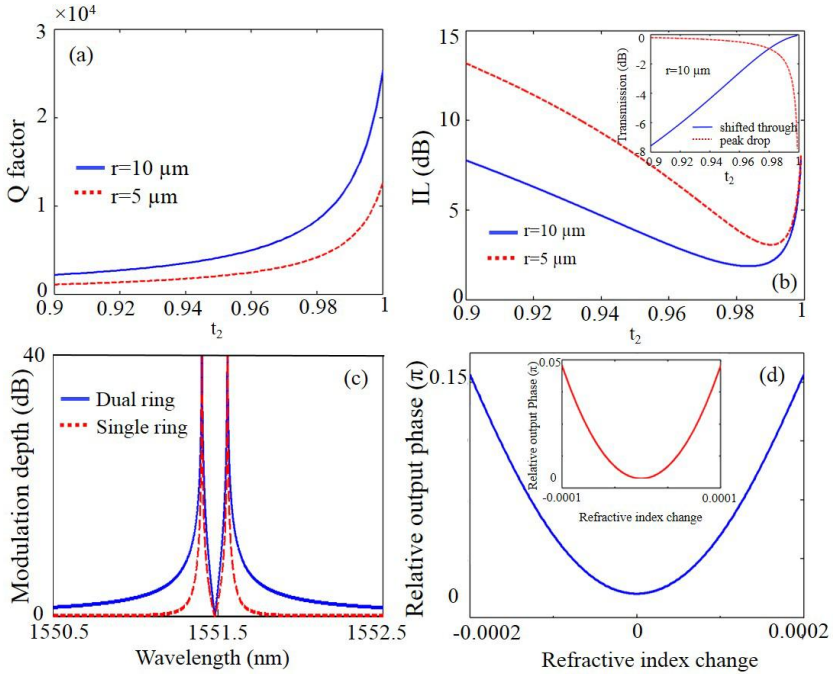

Figure 3. (a) Q factor curves for two ring radii. (b) Insertion loss curves for two ring radii. The inset shows the shifted through transmission of the first ring and the peak drop transmission of the second ring at the wavelength of λ_1. (c) Modulation depth curves for the proposed dual-ring modulator and the single add-drop ring modulator. (d) Output phase in response to reflective index modulation of ±0.0002 in a push-pull manner. The inset shows a smaller reflective index modulation range of ±0.0001.

Fig. 3(a) shows the Q factor curves for two ring radii. The Q factor increases with t_2, which limits the modulation speed. The modulation depth, defined as the power ratio between the "1" and "0" levels, is high due to the near zero transmission of the through-port of one ring at the critical coupling. A relatively low-Q ring is preferred as its cavity lifetime-limited bandwidth is large. The modulator insertion loss (IL) is defined as the loss of the "1" level. From Fig. 2, it can be seen that the IL is affected by both the shifted through transmission of the first ring and the peak drop transmission of the second ring assuming the operation wavelength is λ_1. Fig. 3(b) shows the IL as a function of t_2 for two ring radii. The IL first decreases and then increases with t_2. It reaches the minimum value of 1.87 dB at t_2=0.984 for the larger ring with r=10 μm, which is due to the optimal value given by the multiplication of the shifted through and the peak drop transmission at the wavelength of λ_1, as shown in the inset in Fig. 3(b). The IL of the larger ring is less sensitive to t_2 than that of the smaller ring. Fig. 3(c) shows the modulation depth curves for the proposed dual-ring resonator and the single add-drop ring resonator (through-port as the modulator output). The bandwidth of the dual-ring resonator is wider than the single-ring, leading to a higher tolerance to operation wavelength shift. In the conventional single-ring modulators, chirp is an inevitable feature since the phase change of the active waveguide induces the varied output phase with time. In this structure, the modulator is driven in a push-pull manner, and therefore the phase change from either ring is similar but in an opposite direction by setting the operation wavelength slightly blue-shifted from λ_1 or red-shifted from λ_2. In this way, the frequency chirp of the modulated signals can be highly suppressed. Fig. 3(d) shows the output phase with the push-pull refractive index change. The end points of the output phase curve correspond to the two modulation levels. The device parameters are set as a=0.995, r =10 μm, t_2=t_4=0.98, t_1=t_3=at_2, and Δn_{eff} =±0.0002. The output phase varies within 0.15π, smaller than a regular ring. Furthermore, if Δn_{eff} decreases to ±0.0001, the output phase variation is approximately equal to zero, leading to nearly chirp-free modulation. In this case, the IL is a little higher around 3.9 dB.

3. DUAL-RING MODULATOR IN A PARALLEL CONFIGURATION

Coupled ring resonators in a parallel configuration can be employed with many unique features, such as 'box'-like optical bandpass spectrum [10], Vernier effect-induced FSR expansion [11] and EIT-like resonance profiles [9]. During the push-pull modulation, the parallel coupled ring resonators presented here open a new way to realize EIT-based high-speed modulation.

Fig. 4 shows the schematic diagram of ring resonators coupled in the parallel configuration. t_i and k_i with i= 1, 2, 3, 4 are the transmission and coupling coefficients of the four directional couplers, respectively. L_w is the distance between the centers of two rings, a is the loss factor, and r is the ring radius. We assume that both rings (R_1 and R_2) are identical and operate in the critical coupling regime, but aren't directly coupled to each other.

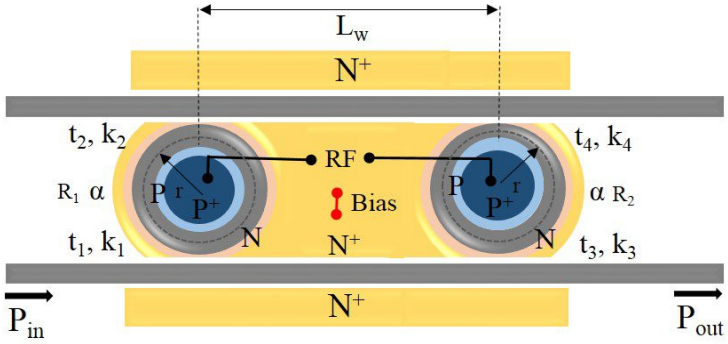

Figure 4. Schematic illustration of the dual ring resonators coupled in the parallel configuration.

Fig. 5(a) shows the optical transmission spectra for various Δn_{eff}. The device parameters are set as a=0.995, r=10 μm, t_2=t_4=0.98, t_1=t_3=at_2=at_4, L_w=$m\pi r$ (m=1). When Δn_{eff}=0, the resonances of both rings are accurately aligned. Light is completely coupled into both rings, and therefore the rings act like mirrors to reflect all light from one waveguide to the other. A deep narrow notch is present in the transmission spectrum, corresponding to the "0" level of the modulated signal. At the other modulation state, the rings are driven in a push-pull mode. The resonances of the rings shift in opposite directions and the original deep notch gradually splits into two. When Δn_{eff} is small (Δn_{eff} = 0.00005 for example), the two rings form a Fabry-Perot (FP)-like cavity, enabling the light traveling in the waveguides between the two rings to generate a EIT-like narrow peak in the original deep valley. As Δn_{eff} increases to a larger value (Δn_{eff}= 0.0005 for example), both rings are far away from the original resonances, and light is transmitted through without coupling to the rings. The full transmission at the original resonance wavelength corresponds to the "1" level of the modulated signal.

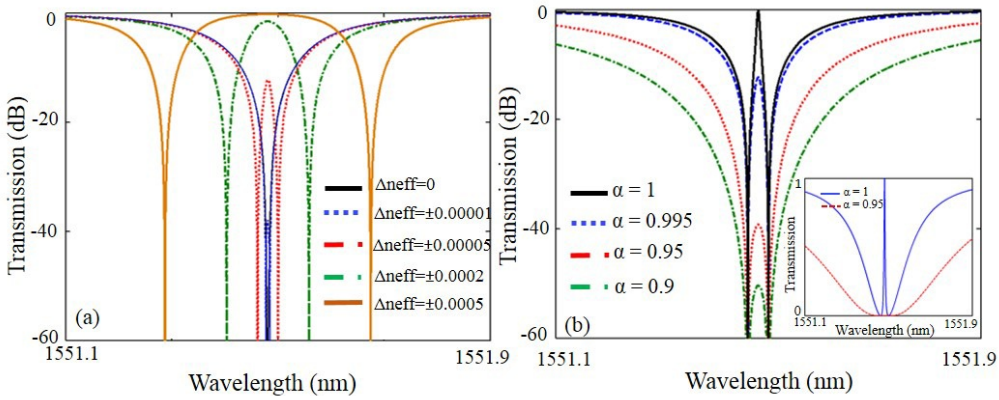

Figure 5. (a) Optical transmission spectra of the dual-ring resonators in the parallel configuration for various refractive index changes. (b) Optical transmission spectra for various loss factors. Here, t_2 =0.98, and Δn_{eff}= 0.00005. The inset shows the transmission in a linear scale for better clarity.

Note that the EIT peaks are very narrow and sharp, extremely sensitive to the loss factor a, as shown in Fig. 5(b). For better clarity, the optical transmission spectra with a linear y-axis are shown in the inset. The peak is strongly suppressed and almost unnoticeable when a decreases from 1 to 0.95.

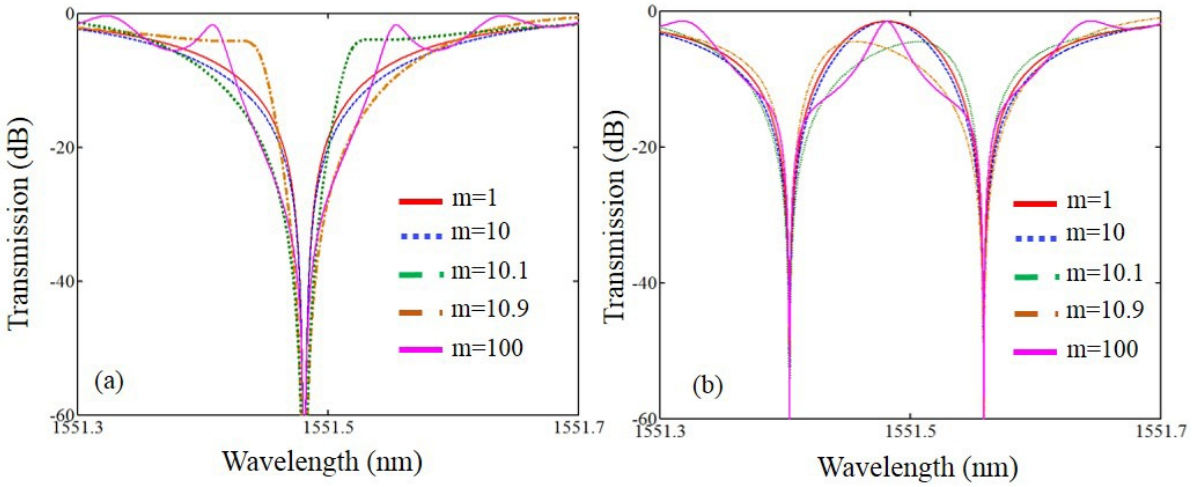

Figure 6. Optical transmission spectra of the coupled resonators in the parallel configuration for various m values at the (a) "0" level of the modulated signal, (b) "1" level of the modulated signal. Here, t_2 =0.98, and a =0.995.

The distance between the ring centers (L_w) also plays an important role in the overall frequency response. Fig. 6(a) shows the optical transmission spectra at the "0" level state. When m is an integer (1, 10 and 100 as examples), the optical transmission spectra are symmetric. It should be noted that ripples appear in the spectrum when m is large. In contrast, when m is a non-integer (10.1 and 10.9 as examples), the optical transmission spectra are asymmetric. At the "1" level state, a peak appears at the original resonance wavelength when m is an integer, and shifts slightly aside when m is a non-integer, as shown in Fig. 6(b). In order to get a more compact size and a lower IL, a smaller integer m should be adopted.

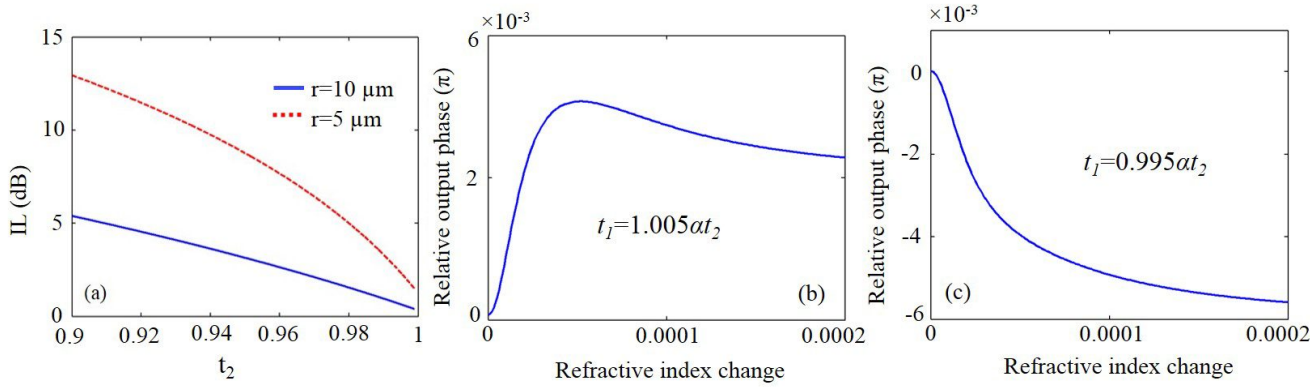

Figure 7. (a) Insertion loss as a function of t_2 for two ring radii. (b) and (c) Output phase as a function of push-pull refractive index change with the rings in (b) under-coupling regime and (c) over-coupling regime.

Fig. 7(a) shows the IL as a function of t_2 for two ring radii. We assume a=0.995, m=1, and Δn_{eff}=±0.0002. The IL decreases with t_2 for both ring radii, and the IL of the larger ring is less sensitive to t_2 than that of the smaller ring. In particular, when t_2=0.98, an IL of 1.5 dB can be achieved with a high modulation depth. The frequency chirp of the modulated signals can be highly suppressed by letting the rings slightly deviate from critical coupling, as shown in Figs. 7(b) and 7(c). The IL of around 1.5 dB and modulation depth of around 28 dB can be achieved in both cases.

4. CONCLUSIONS

In summary, we have presented and analyzed two types of dual-ring modulators with the two microrings cascaded either in series or in parallel. With the serial configuration, low through transmission of one ring and shifted drop transmission of the other ring correspond to the modulation “0” state, while shifted through transmission of one ring and the peak drop transmission of the other ring correspond to the modulation “1” state. Under the parallel configuration, a deep notch in the spectrum resulted from the critical coupling of both rings present the “0” state of the modulated signal, while the EIT peak upon shifting the two rings oppositely generates the “1” state. The frequency chirp of the modulated signals can be highly suppressed owing to the push-pull modulation of the two rings.

ACKNOWLEDGMENT

This work was supported by the Alexander von Humboldt Foundation.

REFERENCES

[1] Reed, G. T., Mashanovich, G., Gardes, F. Y. and Thomson, D. J., "Silicon optical modulators," Nature photonics 4, 518-526 (2010).

[2] Li, Z. Y., Xu, D. X., McKinnon, W. R., Janz, S., Schmid, J. H., Cheben, P. and Yu, J. Z., "Silicon waveguide modulator based on carrier depletion in periodically interleaved PN junctions," Optics Express 17, 15947-15958 (2009).

[3] Ding, J. F., Chen, H. T., Yang, L., Zhang, L., Ji, R. Q., Tian, Y. H., Zhu, W. W., Lu, Y. Y., Zhou, P., Min, R. and Yu, M. B., "Ultra-low-power carrier-depletion Mach-Zehnder silicon optical modulator," Optics Express 20, 7081-7087 (2012).

[4] Saadi, A. A., Franke, B. A., Kupijai, S., Theiss, C., Rhee, H., Mahdi, S., Zimmermann, L., Stolarek, D., Richter, H. H., Eichler, H. J., Woggon, U., Meister, S., "Performance improvement of silicon micro-cavity modulators by iteration of the p-i-n intrinsic region width," in Proceedings of ECOC 2013, London, paper We.1.B.3 (2013).

[5] Zhou, L. J., and Poon, A. W., "Silicon electro-optic modulators using pin diodes embedded 10-micron-diameter microdisk resonators," Optics Express 14, 6851-6857 (2006).

[6] Li, Y. C., Zhang, L., Song, M. P., Zhang, B., Yang, J.-Y., Beausoleil, R. G., Willner, A. E. and Dapkus, P. D., "Coupled-ring-resonator-based silicon modulator for enhanced performance," Optics Express 16, 13342-13348 (2008).

[7] Zhou, L. J., Chen, H., and Poon, A. W., "NRZ-to-PRZ format conversion using silicon second-order coupled-microring resonator-based notch filters," in Proceedings of CLEO/QELS 2007, Maryland, paper CTHP4 (2007).

[8] Zhou, L.J., Ye, T. and Chen, J. P., "Coherent interference induced transparency in self-coupled optical waveguide-based resonators," Optics letters, 36, 13-15 (2011).

[9] Xu, Q. F., Shakya, J. and Lipson, M., "Direct measurement of tunable optical delays on chip analogue to electromagnetically induced transparency," Optics Express 14, 6463-6468 (2006).

[10] Mancinelli, M., Guider, R., Bettotti, P., Masi, M., Vanacharla, M. R., Fedeli, J. –M., Thourhout, D. V., Pavesi, L., "Optical characterization of silicon-on-insulator–based single and coupled racetrack resonators," Journal of Nanophotonics 5, 051705-1-051705-8 (2011).

[11] Schwelb, O. and Frigyes, I., "A design for a high finesse parallel- coupled microring resonator filter," Microwave and Optical technology 38, 125 - 129 (2003).